Supporting Information

Shear-triggered Crystallization and Light Emission of a Thermally Stable Organic Supercooled Liquid

Kyeongwoon Chung,[1] Min Sang Kwon,[2] Brendan M. Leung,[3] Antek G. Wong-Foy,[4] Min Su Kim,[7] Jeongyong Kim,[7,8] Shuichi Takayama,[1,3,6] Johannes Gierschner,[9] Adam J. Matzger,[1,4] and Jinsang Kim[1,2,3,4,5,6]∗

[1]Macromolecular Science and Engineering, University of Michigan, Ann Arbor, MI 48109, USA.

[2]Department of Materials Science and Engineering, University of Michigan, Ann Arbor, MI 48109, USA.

[3]Department of Biomedical Engineering, University of Michigan, Ann Arbor, MI 48109, USA.

[4]Department of Chemistry, University of Michigan, Ann Arbor, MI 48109, USA.

[5]Department of Chemical Engineering, University of Michigan, Ann Arbor, MI 48109, USA.

[6]Biointerfaces Institute, University of Michigan, Ann Arbor, MI 48109, USA.

[7]Center for Integrated Nanostructure Physics, Institute for Basic Science (IBS), Sungkyunkwan University, Suwon 440-746, Republic of Korea

[8]Department of Energy Science, Sungkyunkwan University, Suwon 440-746, Republic of Korea

[9]Madrid Institute for Advanced Studies, IMDEA Nanoscience, Calle Faraday 9, Campus Cantoblanco, 28049 Madrid, Spain.

*Correspondence to: jinsang@umich.edu

- Number of SI pages: 21
- Number of SI figures: 9
- Number of SI tables: 3
- Number of SI movies: 5
- Number of SI data: 2

■ Methods

Spectroscopic Characterization ^{1}H-NMR spectrum was characterized by a Varian, Inova 500 (500 MHz) in $CDCl_3$ solution. ^{13}C-NMR spectrum was recorded on a Varian, MR400 (400 MHz) in $CDCl_3$ solution. Chemical shift values were recorded as parts per million relative to tetramethylsilane as an internal standard. Coupling constants were recorded in Hertz. Mass spectra were recorded on an Agilent Q-TOF 6520 system using electrospray in positive ion detection (ESI+) mode. Photoluminescence, absolute quantum yield and time-resolved fluorescence lifetime were obtained using PTI QuantaMasterTM spectrofluorometers equipped with an integrating sphere and a Laser excitation system. The relative fluorescence quantum yield was measured using Rhodamine 6G in ethanol as a standard reference (1×10^{-7} mol·L^{-1}, Φ_{PL} = 95%).[1] UV-visible absorption spectra were measured on a Varian Cary50 UV/Vis spectrophotometer.

Computational Details The compounds were geometry optimized in *vacuo* by density functional theory (DFT) imposing C_i symmetry. Dimer pair calculations were done by replacing the dimer pairs of adjacent molecules in the x-ray analysis by density functional theory (DFT)-optimized ones. Vertical transition energies of the single molecules, dimer and tetramer configurations were calculated at the time-dependent (TD-)DFT level of theory. All calculations were done employing the standard B3LYP functional and 6-311G* basis set as defined in the Gaussian09 program package. Alternatively, vertical transitions were calculated by the semiempirical intermediate neglect of differential overlap (INDO) method as parameterized by Zerner for spectroscopic applications ZINDO/S, taking into account full single configuration interaction (SCI) over the occupied and unoccupied π-type molecular orbitals (MOs).

Gaussian 09, Revision A.02, M. J. Frisch, G. W. Trucks, H. B. Schlegel, G. E. Scuseria, M. A. Robb, J. R. Cheeseman, G. Scalmani, V. Barone, B. Mennucci, G. A. Petersson, H. Nakatsuji,

M. Caricato, X. Li, H. P. Hratchian, A. F. Izmaylov, J. Bloino, G. Zheng, J. L. Sonnenberg, M. Hada, M. Ehara, K. Toyota, R. Fukuda, J. Hasegawa, M. Ishida, T. Nakajima, Y. Honda, O. Kitao, H. Nakai, T. Vreven, J. A. Montgomery, Jr., J. E. Peralta, F. Ogliaro, M. Bearpark, J. J. Heyd, E. Brothers, K. N. Kudin, V. N. Staroverov, R. Kobayashi, J. Normand, K. Raghavachari, A. Rendell, J. C. Burant, S. S. Iyengar, J. Tomasi, M. Cossi, N. Rega, J. M. Millam, M. Klene, J. E. Knox, J. B. Cross, V. Bakken, C. Adamo, J. Jaramillo, R. Gomperts, R. E. Stratmann, O. Yazyev, A. J. Austin, R. Cammi, C. Pomelli, J. W. Ochterski, R. L. Martin, K. Morokuma, V. G. Zakrzewski, G. A. Voth, P. Salvador, J. J. Dannenberg, S. Dapprich, A. D. Daniels, Ö. Farkas, J. B. Foresman, J. V. Ortiz, J. Cioslowski, and D. J. Fox, Gaussian, Inc., Wallingford CT, 2009.

Cell Experiments Details For phenyltrichlorosilane (PTS) treatment, glass substrates were cleaned by sonication in a sequence of water, acetone, chloroform and isopropanol. Cleaned glass substrates were dipped in the piranha solution for 6 min at 100 ^{o}C followed by sonication in water and isopropanol. After baking in vacuum oven (60 ^{o}C, 1 hr), substrates were under UV/O_3 treatment for 20 min (UV/Ozone ProCleaner, BioForce Nanosciences). Substrates were dipped in PTS (1.5 ml) in toluene solution (60 ml) for 30 min at 60 ^{o}C followed by sonication in toluene and isopropanol. PTS treated substrates were stored under vacuum oven for 1 hr before spincasting of DPP8 in chlorobenzene solution. Prepared supercooled liquid DPP8 films were annealed at 150 ^{o}C to remove residual solvents before cell seeding. Human bone marrow fibroblast (HS-5) were purchased from the American Type Culture Collection (ATCC# CRL-11882). Cells were cultured in Dulbecco's Modified Eagle's Medium (Gibco cat#11995-065) supplemented with 10% fetal bovine serum (Gibco cat#16000044) and 1% antibiotic-antimycotic (Gibco cat#15240-062). Stock culture and subsequent cell seeded samples were maintained in a humidified (100%), 37 ^{o}C, CO_2 incubator (5% CO_2, 95% air). At time of seeding, HS-5 cells were trypsinized and seeded on

supercooled liquid DPP8 film at a density of ca, 10^3 cells·cm^{-2}. Prior to seeding, supercooled liquid DPP8 films were treated with fibronectin solution (10 μg·mL^{-1}) to enhance cell attachment. After 2-day incubation, cells were visualized using an Olympus BX51 microscope equipped with a UV/vis excitation system for bright field and fluorescence imaging.

Powder X-ray Diffraction and Thermal Analysis Powder X-ray diffraction (PXRD) patterns of DPP derivatives (Figure 3C) were collected at ambient temperature using a Rigaku R-AXIS SPIDER diffractometer with an imaging plate detector using graphite monochromated Cu-Kα radiation (λ=1.54 Å). Samples were mounted on a nylon cryoloop. To obtain powder patterns with minimized preferred orientation, images were collected for 5 minutes while rotating the sample about the φ-axis at 10°·s^{-1} while oscillating ω between 120° and 180° at 1°·s^{-1} with χ set at 45°. Images were integrated in AreaMax (2.0.0.4 ed., Rigaku, 2005) software package with a step size of 0.1° to generate 2θ versus intensity data. The resulting powder patterns were processed in Jade 9+ (Ver. 9.5.0) to calculate peak positions and intensities. PXRD patterns in Figure S6 were collected at room temperature using a Rigaku rotating anode x-ray diffractometer. Powder samples were securely placed into a special quartz holder. Cu-Kα radiation (λ=1.54 Å) source generated from a 12 kW Rigaku rotating anode generator that was operated at 40 kV and 100 mA. The powder diffraction profiles were measured in the 2θ range from 2º to 40º (step size 0.02º). The resulting powder patterns were analyzed using Origin software (OriginPro 8, OriginLab Corp., Northampton, MA, USA) to define peak positions and intensities. The thermal properties of samples were measured using differential scanning calorimetry (DSC) of TA Instruments Discovery DSC (Figure 2 and Figure 3D) and Perkin Elmer DSC7 (Figure 3A and Figure S2).

Single Crystal Structure Analysis for DPP8 Orange blocks of DPP8 were grown from an acetonitrile solution of the compound at 23 ^{o}C. A crystal of dimensions 0.14 × 0.10 × 0.02

mm was mounted on a Rigaku AFC10K Saturn 944+ CCD-based X-ray diffractometer equipped with a low temperature device and Micromax-007HF Cu-target micro-focus rotating anode (λ = 1.54187 Å) operated at 1.2 kW power (40 kV, 30 mA). The X-ray intensities were measured at 85(1) K with the detector placed at a distance 42.00 mm from the crystal. A total of 4224 images were collected with an oscillation width of 1.0^{o} in ω. The exposure time was 5 sec. for the low angle images, 35 sec. for high angle. The integration of the data yielded a total of 92579 reflections to a maximum 2θ value of 136.48^{o} of which 5914 were independent and 5496 were greater than 2σ(I). The final cell constants (Table S1) were based on the xyz centroids 55569 reflections above 10σ(I). Analysis of the data showed negligible decay during data collection; the data were processed with CrystalClear 2.0 and corrected for absorption. The structure was solved and refined with the Bruker SHELXTL (version 2008/4) software package, using the space group P2(1)/c with Z = 4 for the formula $C_{34}H_{42}N_2O_2Br_2$. All non-hydrogen atoms were refined anisotropically with the hydrogen atoms placed in idealized positions. Full matrix least-squares refinement based on F^2 converged at R_1 = 0.0431 and wR_2 = 0.1090 [based on I > 2σ(I)], R_1 = 0.0453 and wR_2 = 0.1107 for all data. Additional details are presented in Table S1 and are given as a CIF file (Supplementary Data 1, CCDC deposition number 1016376).

Sheldrick, G.M. SHELXTL, v. 2008/4; Bruker Analytical X-ray, Madison, WI, 2008.

CrystalClear Expert 2.0 r12, Rigaku Americas and Rigaku Corporation (2011), Rigaku Americas, 9009, TX, USA 77381-5209, Rigaku Tokyo, 196-8666, Japan.

Single Crystal Structure Analysis for DPP4 Orange prismatic crystals of DPP4 were grown from an ethanol solution of the compound at 22 ^{o}C. A crystal of dimensions 0.14 × 0.09 × 0.08 mm was mounted on a Rigaku AFC10K Saturn 944+ CCD-based X-ray diffractometer equipped with a low temperature device and Micromax-007HF Cu-target micro-focus rotating anode (λ= 1.54187 A) operated at 1.2 kW power (40 kV, 30 mA). The X-ray intensities were

measured at 85(1) K with the detector placed at a distance 42.00 mm from the crystal. A total of 4031 images were collected with an oscillation width of 1.0^{o} in ω. The exposure time was 2 sec. for the low angle images, 12 sec. for high angle. The integration of the data yielded a total of 66066 reflections to a maximum 2θ value of 136.44^{o} of which 4382 were independent and 4207 were greater than 2σ(I). The final cell constants (Table S2) were based on the xyz centroids 47236 reflections above 10σ(I). Analysis of the data showed negligible decay during data collection; the data were processed with CrystalClear 2.0 and corrected for absorption. The structure was solved and refined with the Bruker SHELXTL (version 2008/4) software package, using the space group I2/a with Z = 8 for the formula $C_{26}H_{26}N_2O_2Br_2$. All non-hydrogen atoms were refined anisotropically with the hydrogen atoms placed in idealized positions. Full matrix least-squares refinement based on F^2 converged at R_1 = 0.0241 and wR_2 = 0.0641 [based on I > 2σ(I)], R_1 = 0.0249 and wR_2 = 0.0649 for all data. Additional details are presented in Table S2 and are given as a CIF file (Supplementary Data 2, CCDC deposition number 1016377).

Free Energy Difference ΔG between supercooled liquid and crystalline solid of DPP8 was calculated with three different methods; i.e. by [1] relative solubility measurement,[2] [2] via the Hoffman equation,[3] [3] via a thermodynamic cycle (Hess's law) using Kirchhoff's law inserting the heat capacity (C_p) of supercooled liquid and crystalline solid (Figure S3).

[1] Relative solubility measurements were performed in a previously described manner.[2] The optical absorbance of supercooled liquid and crystal powder in water and methanol mixture solvent (1:7) was measured using Varian Cary50 UV/Vis spectrophotometer. By monitoring the time-dependent absorbance curve, the absorbance at equilibrium was determined. At equilibrium, the ratio of absorption intensity represents equilibrium constant (K_{eq}) in the following equation: $\Delta G = -RT(\ln K_{eq})$. R is gas constant and T is temperature in Kelvin. Inserting K_{eq} = 2.883, the calculated ΔG between supercooled liquid state and crystalline solid

state is ΔG = -2.63 kJ·mol^{-1} (-0.63 kcal·mol^{-1}) at 26 ^{o}C. This free energy difference may represent a slight underestimation due to a conversion of supercooled liquid to crystal form under the experimental conditions.

[2] The Hoffmann equation, $\Delta G = \Delta H_f(T_m\text{-}T)T \cdot T_m^{-2}$, was used for the calculation of ΔG between the two phases of DPP8.[3] T_m = 133.62 ^{o}C and ΔH_f = 29.13 kJ·mol^{-1} were measured by means of Discovery DSC, to give ΔG = -5.67 kJ·mol^{-1} (-1.35 kcal·mol^{-1}) at 26 ^{o}C. This value may slightly deviate from the real value because heat capacity is not considered in the equation.[4]

[3] ΔG was calculated via a thermodynamic cycle (Hess's law) using $\Delta G = \Delta H - T\Delta S$ and Kirchhoff's law by inserting the C_p of the supercooled liquid and the crystalline solid. The calculation procedure is presented in Figure S3. The calculated ΔG = -6.24 kJ·mol^{-1} (-1.49 kcal·mol^{-1}) at 26 ^{o}C may be slightly overestimated due to additional heat capacity contribution from 388 K (115 ^{o}C) to melting temperature 407 K (134 ^{o}C).

Sonication-triggered nucleation A probe sonicator controlled by Cole Parmer ultrasonic processor and a vial having supercooled liquid DPP8 on the bottom were placed in a water bath as shown in Figure S4. Sonication was conducted for 10 minutes at 29 ^{o}C. To reduce temperature increase of water bath by sonication, sonicator was stopped for 20 sec after every 40 sec sonication. After sonication, the temperature of the water bath was 31 ^{o}C. Supercooled liquid sample treated under sonication was annealed on a hot plate (120 ^{o}C) for 5 minutes and observed under 365 nm UV light to examine nucleation and crystallization.

Heterogeneous nucleation test Sea sand (Fisher Sci.), rubber powders (eraser), or polyimide film (Kapton film, CS Hyde Company) was mixed with molten DPP8 on a glass substrate. To check heterogeneous nucleation and crystallization propagation, the sample was cooled down to room temperature and subsequently heated to 120 ^{o}C. After holding at 120 ^{o}C for 5 minutes, a fluorescence image of the sample was taken. During the whole process the sample was

observed using an Olympus BX51 microscope equipped with a UV/vis excitation system for bright field and fluorescence imaging.

Sensitivity of shear-triggered crystallization Threshold shear rate and shear stress were characterized using ARES Rheometer (TA instruments) equipped with an air forced convection oven. DPP8 crystalline powder was sandwiched between 8 mm diameter parallel plates, and melted at 150 ^{o}C. After cooling down to room temperature, the gap between the two plates was finely adjusted to fill the space between the two plates completely. Under each shear rate from 0.001 to 10 s^{-1}, steady single point test was conducted and corresponding applied shear stress was measured, followed by heating to 100 ^{o}C to confirm nucleation by the shearing. Photographs were taken after subsequent heating under room light.

■ Materials and Synthesis

All starting materials and solvents for the synthesis were purchased from commercial suppliers (Sigma-Aldrich Chemical Co. and Fisher Sci.).

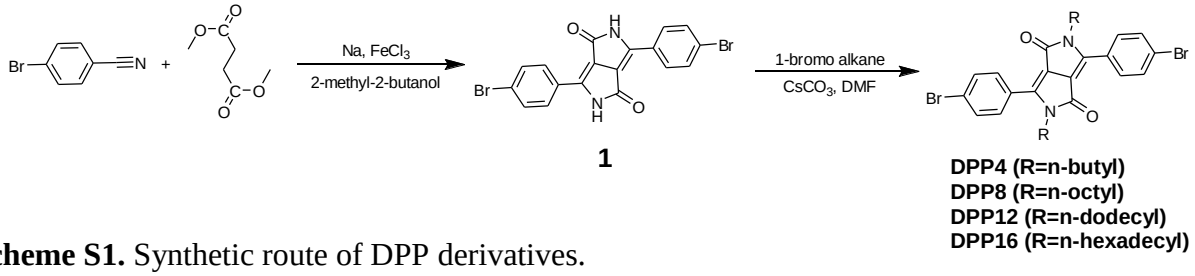

Scheme S1. Synthetic route of DPP derivatives.

3,6-bis(4-bromophenyl)pyrrolo[3,4-c]pyrrole-1,4(2H,5H)-dione. [1] Synthesis of [1] was performed in a previously described manner.[5] Under Ar condition, Sodium (1.26 g, 54.94 mmol) and $FeCl_3$ (0.06 g) was added to dry 2-methyl-2-butanol (27.5 ml) (at room temperature), and the mixture was stirred at 90 ^{o}C. After Sodium is completely dissolved, 4-

bromobenzonitrile (5 g, 27.47 mmol) was added at 50 ^{o}C. At 90 ^{o}C, dimethyl succinate (2.22 g, 10.99 mmol) in 11.5 ml of 2-methyl-2-butanol was added drop wise. The mixture was stirred at 90 ^{o}C for 24 hr. Acetic acid (11.5 ml) was added drop wise to the mixture and was stirred at 120 ^{o}C for 1hr. The reaction mixture was cooled down to room temperature and filtered. The filtered dark red solid was washed with hot water and hot methanol several times and used for next reaction without further purification. Product 2.29 g, (47%).

3,6-bis(4-bromophenyl)-2,5-dioctylpyrrolo[3,4-c]pyrrole-1,4(2H,5H)-dione. (DPP8)

Under Ar condition, 3,6-bis(4-bromophenyl)pyrrolo[3,4-c]pyrrole-1,4(2H,5H)-dione (1 g, 2.24 mmol), Cs_2CO_3 (2.191 g, 6.72 mmol) and 1-bromooctane (1.73 g, 8.97 mmol) was added in dry dimethylformamide (25 ml). The mixture was stirred at 40 ^{o}C for 24 hr. After cooling to room temperature, the mixture was poured into water and extracted with chloroform. The organic phase was dried over $MgSO_4$ and the solvent was evaporated in *vacuo*. Column chromatography (dichloromethane as eluent) and multiple recrystallizations (methanol or ethanol) were performed. Orange crystal of DPP8 was obtained. Product 0.65 g (43%). ^{1}H NMR (500 MHz, CDCl3): δ 7.71 – 7.65 (m, 8 H), 3.72 (t, J=9.3 Hz, 4 H), 1.58 (m, 4H), 1.26 – 1.19 (m, 20H), 0.86 (t, J=8.4 Hz, 6 H). ^{13}C NMR (400 MHz, CDCl3): δ 162.6, 147.6, 132.3, 130.3, 127.1, 126.0, 110.0, 42.0, 31.9, 29.5, 29.3, 29.2, 26.8, 22.8, 14.3. MS m/z (ESI+, relative intensity): 671 (M^{+}+1, 100), 520 (6), 409 (19), 312 (25). HRMS (ESI+) calcd. for $C_{34}H_{42}Br_2N_2O_2$ (M^{+}+1) 669.1686, found 669.1665.

3,6-bis(4-bromophenyl)-2,5-dibutylpyrrolo[3,4-c]pyrrole-1,4(2H,5H)-dione. (DPP4)

Same procedure with DPP8 was performed. Replacing 1-bromooctane, 1-bromobutane was used. Product 0.46 g (37%). ^{1}H NMR (500 MHz, CDCl3): δ 7.71 – 7.65 (m, 8 H), 3.74 (t, J=9.3 Hz, 4 H), 1.56 (m, 4H), 1.29 – 1.23 (m, 4H), 0.85 (t, J=9.0 Hz, 6 H). ^{13}C NMR (400 MHz, CDCl3): δ 162.5, 147.6, 132.3, 130.3, 127.0, 126.0, 110.0, 41.7, 31.6, 20.1, 13.8. MS

m/z (ESI+, relative intensity): 559 (M^++1, 100), 409 (5). HRMS (ESI+) calcd. for $C_{26}H_{26}Br_2N_2O_2$ (M^++1) 557.0434, found 557.0424.

3,6-bis(4-bromophenyl)-2,5-didodecylpyrrolo[3,4-c]pyrrole-1,4(2H,5H)-dione. (DPP12) Same procedure with DPP8 was performed. Replacing 1-bromooctane, 1-bromododecane was used. Product 0.52 g (30%). ^{1}H NMR (500 MHz, CDCl3): δ 7.71 – 7.65 (m, 8 H), 3.72 (t, J=9.0 Hz, 4 H), 1.56 (m, 4H), 1.29 – 1.19 (m, 36H), 0.88 (t, J=8.4 Hz, 6 H). ^{13}C NMR (400 MHz, CDCl3): δ 162.6, 147.6, 132.4, 130.3, 127.1, 126.0, 110.0, 42.0, 32.1, 29.8, 29.7, 29.6, 29.5, 29.2, 26.9, 22.9, 14.3. MS m/z (ESI+, relative intensity): 783 (M^++1, 45), 576 (23), 409 (100), 298 (24), 186 (19). HRMS (ESI+) calcd. for $C_{42}H_{58}Br_2N_2O_2$ (M^++1) 781.2938, found 781.2911.

3,6-bis(4-bromophenyl)-2,5-dihexadecylpyrrolo[3,4-c]pyrrole-1,4(2H,5H)-dione. (DPP16) Same procedure with DPP8 was performed. Replacing 1-bromooctane, 1-bromohexadecane was used. Product 0.56 g (28%). ^{1}H NMR (500 MHz, CDCl3): δ 7.71 – 7.65 (m, 8 H), 3.72 (t, J=9.3 Hz, 4 H), 1.56 (m, 4H), 1.30 – 1.19 (m, 52H), 0.88 (t, J=8.4 Hz, 6 H). ^{13}C NMR (400 MHz, CDCl3): δ 162.6, 147.6, 132.4, 130.3, 127.1, 126.0, 110.1, 42.0, 32.1, 29.9, 29.9, 29.8, 29.7, 29.6, 29.6, 29.2, 26.9, 22.9, 14.3. MS m/z (ESI+, relative intensity): 895 (M^++1, 49), 752 (28), 708 (45), 664 (57), 576 (68), 532 (60), 488 (38), 408 (100), 298 (66), 242 (85). HRMS (ESI+) calcd. for $C_{50}H_{74}Br_2N_2O_2$ (M^++1) 893.4190, found 893.4166.

■ Homogeneous Nucleation Theory

According to homogeneous nucleation theory,[6] two processes should be accomplished for crystallization, i.e. nucleation and propagation. The Gibbs free energy of nucleation, $\Delta G^{nucleation}$, for a (spherical) nucleus with radius *r* in a supercooled liquid is expressed as the sum of the energy gain by generating an energetically more favorable crystalline nucleus and the energy loss by producing the interface, driven by surface tension (σ).

$$\Delta G^{nucleation} = \frac{4}{3}\pi r^3 \Delta G_v + 4\pi r^2 \sigma \quad [1]$$

For dG/dr = 0, the critical radius of nucleation (r*) is derived, corresponding to the minimum nucleus which can continue growing spontaneously and which is inversely proportional to the Gibbs free energy difference ($\Delta G_v = G_v$(crystal) – G_v(supercooled liquid)) between the supercooled liquid and the crystalline phase. ΔH_v is heat of transformation.

$$r^* = -\frac{2\sigma}{\Delta G_v} \sim -\frac{2\sigma T_m}{\Delta H_v (T_m - T)} \quad [2]$$

If the radius of nuclei is larger than r*, the mobility of the molecules in the liquid phase will determine the growth rate of the crystallization process. According to Equation 2, at small undercooling below T_m, a larger nucleus is necessary for crystallization, but the higher mobility of molecules is favorable for crystal growth. In contrast, as temperature goes further down, while the critical radius r* decreases, which means that even a small nucleus can survive, the mobility of the molecules also decreases, slowing down crystal growth.

- **Photophysical Properties of DPP8**

The PL lifetime, τ_{PL}, and the radiative rate constant ($k_r=\Phi_{PL}/\tau_{PL}$) of the crystalline DPP8 are similar to the solution values (Table S3), which implies a weakly coupled system with no preferential H-or J-type coupling in the solid state.[7] The emission is red-shifted by ca. 700 cm^{-1} (22 nm) against solution (Figure S7), which can be ascribed to the higher polarizability in the crystalline state compared to solution.[8,9] The single crystal structure analysis shows molecular layers kept effectively apart by the long alkyl chains (Figure 2C). Within a layer, nearest neighbors are substantially shifted along the long molecular axis, suggesting weak J-coupling (Figure S8), while second nearest neighbors are side-by-side oriented, giving rise to some H-coupling, so that the effects should cancel each other in a first approximation. This

was examined by quantum chemical calculations of an assembly of four DPP8 molecules, which indicates indeed very weak H-aggregation (Figure S9).[10] Such weakly coupled systems are known to be highly luminescent even in the polycrystalline state,[11] essentially due to reduced exciton diffusion.[12]

In contrast to the crystalline phase, the supercooled liquid DPP8 effectively quenches emission, exhibiting a weak, unstructured and strongly red-shifted excimer-like PL spectrum with a large Stokes shift of 3800 cm^{-1} (130 nm; see Figure S7).[13] According to our photophysical analysis (Table S3), PL quenching caused by two factors; (i) a low radiative rate k_r, reduced by a factor of 10 compared to solution, and (ii) a large rate constant for non-radiative deactivation (k_{nr}), enhanced by a factor of 10 against solution. While these features could be interpreted as typical characteristics of H-aggregation in polycrystalline samples,[12] the absorption spectrum of the supercooled liquid does not support such interpretation. For strong H-aggregates a substantial hypsochromic shift relative to solution is expected,[12] while in the current case a red-shift against solution by ca. 600 cm^{-1} (Figure S7) is observed, which agrees with the expected polarizability effect. In the supercooled liquid, all possible intermolecular orientations may be realized which should enhance effective trapping by exciton migration through a multitude of structural trap states.[12] While the majority of traps might deactivate non-radiatively causing the strong increase of k_{nr}, stacks with strong π-π overlap act as deep traps which give rise to the small radiative rate k_r, and the faint excimeric emission.[12]

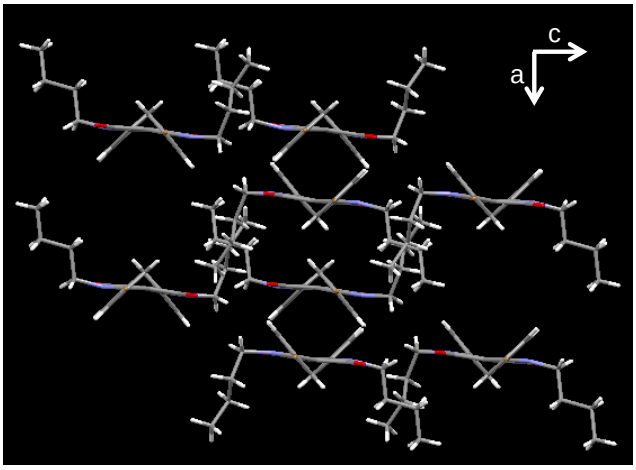

Figure S1. Single crystal structure of DPP4. Closely packed aromatic cores between nearest molecules are clearly observed.

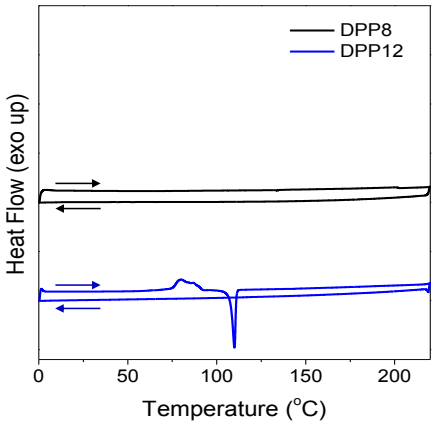

Figure S2. DSC trace (2nd cycle) of DPP8 and DPP12 (scan rate 10 °C·min^{-1} down to 0 °C). While DPP12 did not show any crystallization peak upon subsequent heating when it was cooled down to 20 °C (Figure 3A), onset of crystallization peak was observed at 57 °C upon subsequent heating when DPP12 was cooled down to 0 °C.

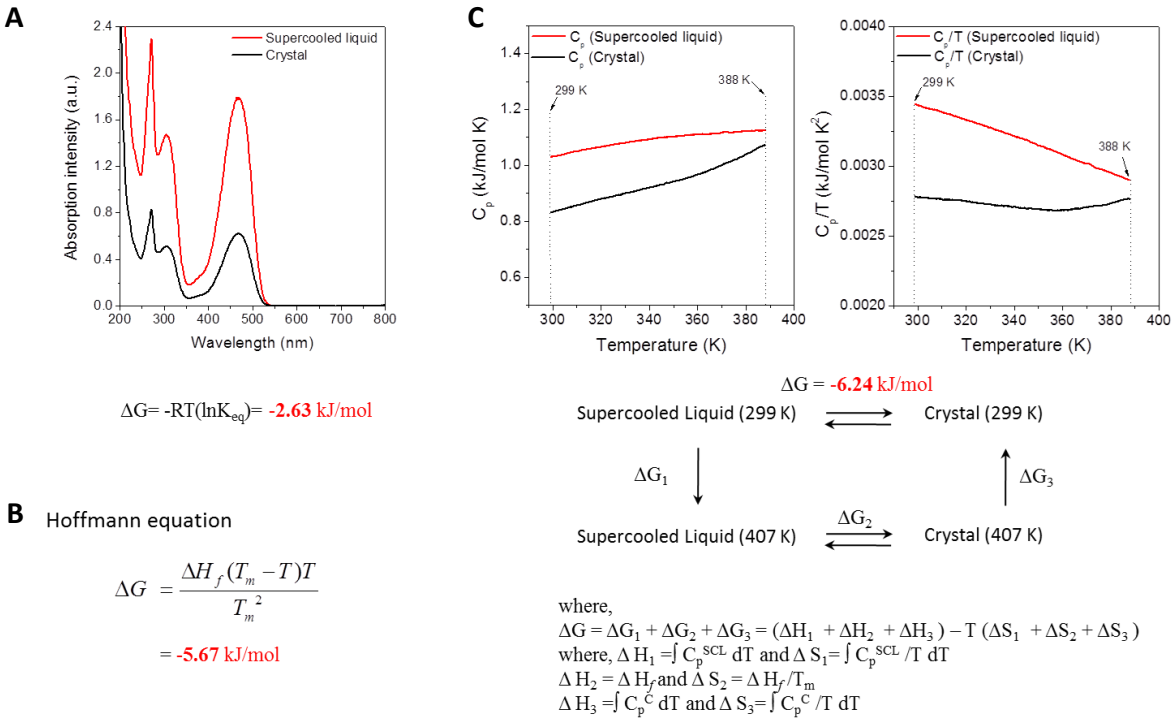

Figure S3. Methods for calculation of ΔG between supercooled liquid and crystalline solid of DPP8. (A) Relative solubility measurement for ΔG calculation. UV-vis absorption spectra of crystal solution and supercooled liquid solution at equilibrium were collected for ΔG calculation (Solvent: water in methanol (1:7)). The ratio of the absorption intensities represents the equilibrium constant (K_{eq}) in the following equation: $\Delta G = -RT(\ln K_{eq})$. The calculated ΔG between supercooled liquid state and crystalline solid state is -2.63 kJ·mol^{-1} at 26 ^{o}C (-0.63 kcal·mol^{-1}). This value may be slightly underestimated due to the observed crystallization of small fraction of supercooled liquid under the experimental conditions. (B) ΔG calculation from Hoffmann equation. T_m and ΔH_f were measured by means of Discovery DSC. Calculated ΔG is -5.67 kJ·mol^{-1} at 26 ^{o}C (-1.35 kcal·mol^{-1}). This value may slightly deviate from the real value because heat capacity is not considered in the equation. (C) ΔG calculation considering heat capacity (C_p) of supercooled liquid and crystalline solid. The calculation procedure is presented in the figure. The calculated ΔG is -6.24 kJ·mol^{-1} at 26 ^{o}C (-1.49 kcal·mol^{-1}) may be slightly overestimated due to additional heat capacity contribution from 388 K (115 ^{o}C) to melting temperature 407 K (134 ^{o}C).

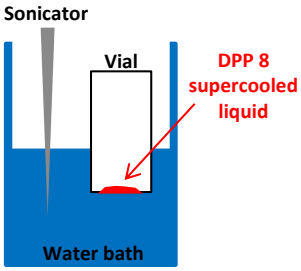

Figure S4. Schematic representation of the sonication experiment setting in order to verify molecular agitation effect on nucleation and crystallization of supercooled liquid DPP8.

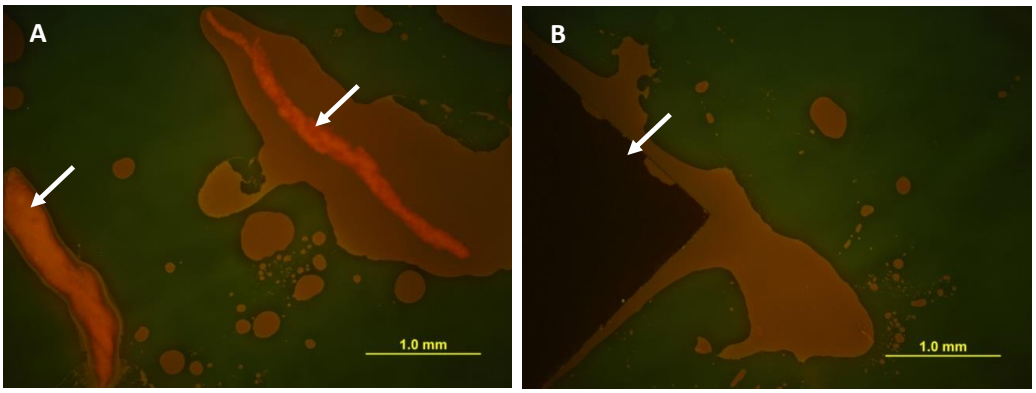

Figure S5. Heterogeneous nucleation test with hydrophobic foreign interfaces. (A) Eraser powders (white arrows) and (B) a piece of polyimide film (white arrow) were mixed with DPP8 melt followed by cooling to 25 ^{o}C and subsequent heating to 120 ^{o}C. Fluorescence images under optical microscope were taken after 5 min at 120 ^{o}C.

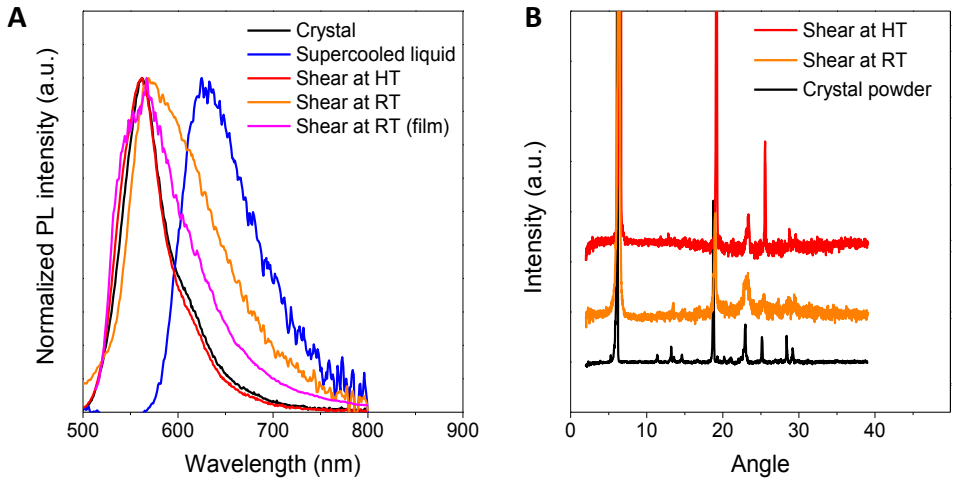

Figure S6. PL spectrum and X-ray diffraction (XRD) patterns of supercooled liquid, crystalline powder and shear-triggered crystal of DPP8. (A) PL spectrum. (B) XRD patterns. (HT= 120 ^{o}C, RT= 25 ^{o}C).

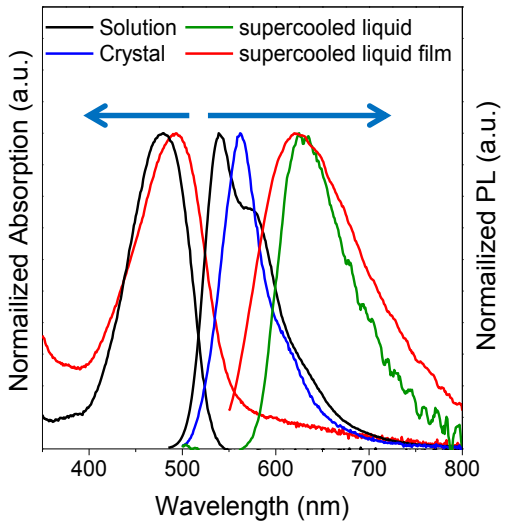

Figure S7. Normalized absorption and emission spectra of solution, crystalline solid and supercooled liquid of DPP8.

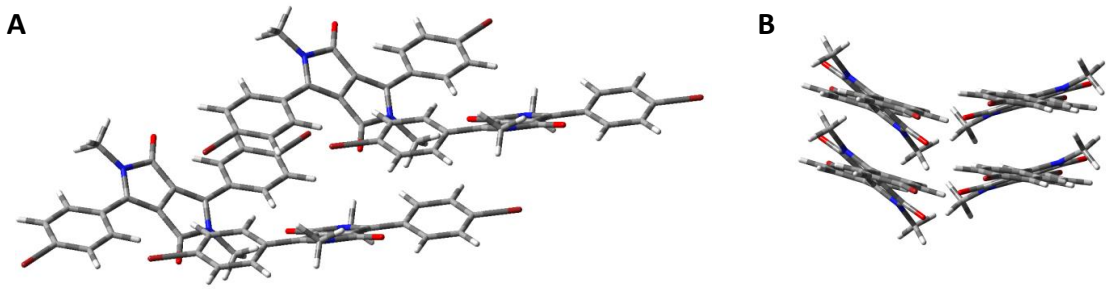

Figure S8. An assembly of four DPP8 molecules taken from the crystal structure (alkyl chains omitted). (A) Side view. (B) Top view.

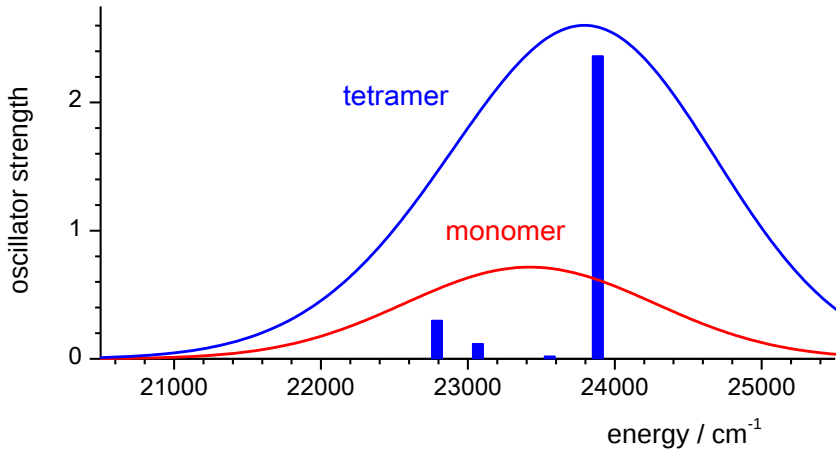

Figure S9. Calculated absorption spectra (ZINDO//DFT) of DPP8 molecule (red) and an assembly of four DPP8 molecules (as taken from the crystal structure; blue).

Table S1. Crystal data and structure refinement for DPP8

Identification code	DPP8
Empirical formula	$C_{34}H_{42}Br_2N_2O_2$
Formula weight	670.52
Temperature	85(2) K
Wavelength	1.54178 Å
Crystal system, space group	Monoclinic, P2(1)/c
Unit cell dimensions	a = 8.9169(2) Å alpha = 90 deg. b = 13.1897(2) Å beta = 92.083(7) deg. c = 27.4851(19) Å gamma = 90 deg.
Volume	3230.4(2) $Å^3$
Z, Calculated density	4, 1.379 Mg/m^3
Absorption coefficient	3.422 mm^{-1}
F(000)	1384
Crystal size	0.14 x 0.10 x 0.02 mm
Theta range for data collection	3.72 to 68.24 deg.
Limiting indices	-10<=h<=10, -15<=k<=15, -32<=l<=33
Reflections collected / unique	92579 / 5914 [R(int) = 0.0834]
Completeness to theta = 68.24	100.00%
Absorption correction	Semi-empirical from equivalents
Max. and min. transmission	0.934 and 0.703
Refinement method	Full-matrix least-squares on F^2
Data / restraints / parameters	5914 / 0 / 363
Goodness-of-fit on F^2	1.072
Final R indices [I > 2σ(I)]	R_1 = 0.0431, wR_2 = 0.1090
R indices (all data)	R_1 = 0.0453, wR_2 = 0.1107
Largest diff. peak and hole	1.097 and -1.195 $e.A^{-3}$

Table S2. Crystal data and structure refinement for DPP4

Identification code	**DPP4**
Empirical formula	**$C_{26}H_{26}Br_2N_2O_2$**
Formula weight	**558.31**
Temperature	**85(2) K**
Wavelength	**1.54178 Å**
Crystal system, space group	**Monoclinic, I2/a**
Unit cell dimensions	**a = 15.3997(3) Å alpha = 90 deg.**
	b = 18.3154(3) Å beta = 91.348(6) deg.
	c = 16.9365(12) Å gamma = 90 deg.
Volume	**4775.6(4) $Å^3$**
Z, Calculated density	**8, 1.553 Mg/m^3**
Absorption coefficient	**4.508 mm^{-1}**
F(000)	**2256**
Crystal size	**0.14 x 0.09 x 0.08 mm**
Theta range for data collection	**3.55 to 68.22 deg.**
Limiting indices	**-18<=h<=18, -22<=k<=21, -20<=l<=20**
Reflections collected / unique	**66066 / 4382 [R(int) = 0.0550]**
Completeness to theta = 68.22	**100.00%**
Absorption correction	**Semi-empirical from equivalents**
Max. and min. transmission	**0.7144 and 0.5710**
Refinement method	**Full-matrix least-squares on F^2**
Data / restraints / parameters	**4382 / 0 / 291**
Goodness-of-fit on F^2	**1.058**
Final R indices [I > 2σ(I)]	**R_1 = 0.0241, wR_2 = 0.0641**
R indices (all data)	**R_1 = 0.0249, wR_2 = 0.0649**
Largest diff. peak and hole	**0.343 and -0.485 $e.A^{-3}$**

Table S3. Optical and photophysical data of DPP8. Absorption and emission maxima, PL lifetimes (τ_{PL}) and quantum yields (Φ_{PL}), rate constants for radiative (k_r) and non-radiative deactivation (k_{nr}), calculated from $\Phi_{PL} = k_r \cdot \tau_{PL} = k_r \cdot (k_r + k_{nr})^{-1}$

System		λ_{abs} / nm	λ_{em} / nm	Stokes shift / cm^{-1}	Φ_{PL}	τ_{PL} / ns	k_r / ns^{-1}	k_{nr} / ns^{-1}
Solution	$CHCl_3$	479	540	2358	0.71[a]	6.05	0.117	0.049
Crystalline solid	powder		562[c]		0.55[b]	4.58	0.120	0.098
	shear (393 K)		562[c]		0.50[b]			
Supercooled liquid	powder		629[c]		0.02[b]	2.13	0.011	0.460
	Powder (77K)				0.18	7.82	0.023	0.105
	film	493	623	4233	0.02[b]	2.35	0.008	0.418

[a] from relative quantum yield measurement against Rhodamine 6G. [b] from absolute measurements in an integrating sphere. [c] subject to reabsorption

Movie S1. Crystallization of supercooled liquid DPP8 upon crystal powder seeding at 120 ^{o}C (under fluorescence optical microscope).

Movie S2. Supercooled liquid DPP8 upon crystal powder seeding at 25 ^{o}C followed by gradual temperature increase to 100 ^{o}C (under fluorescence optical microscope).

Movie S3. Shear-triggered lighting-up crystallization of DPP8 at 120 ^{o}C (under fluorescence optical microscope).

Movie S4. Propagation of DPP8 crystallization at 120 ^{o}C (under fluorescence optical microscope).

Movie S5. Shear-triggered crystals transform back to liquid phase by thermal heating (150 ^{o}C).

Supporting Data 1. Crystallographic data for DPP8 (CIF).

Supporting Data2. Crystallographic data for DPP4 (CIF).

■ References and Notes

(1) Kubin, R. F., and Fletcher, A. N. (1982) Fluorescence quantum yields of some rhodamine dyes. *J. Lumin. 27*, 455–462.

(2) López-mejías, V., Kampf, J. W., and Matzger, A. J. Polymer-Induced Hetenucleation of Tolfenamic Acid : Structural Investigation of a Pentamorph. *J. Am. Chem. Soc. 131*, 4554–4555.

(3) Hoffman, J. D. (1958) Thermodynamic Driving Force in Nucleation and Growth Processes. *J. Chem. Phys. 29*, 1192–1193.

(4) Andronis, V., and Zografi, G. (2000) Crystal nucleation and growth of indomethacin polymorphs from the amorphous state. *J. Non. Cryst. Solids 271*, 236–248.

(5) Zhang, G., Liu, K., Li, Y., and Yang, M. (2009) Novel poly(phenylene ethynylene)-type conjugated polymers containing diketopyrrolopyrrole or triphenylpyrazoline units in the main chain: synthesis, characterization and photophysical properties. *Polym. Int. 58*, 665–673.

(6) Abraham, F. F. (1974) *Homogeneous Nucleation Theory*. Academic Press, New York.

(7) Gierschner, J., and Park, S. Y. (2013) Luminescent distyrylbenzenes: tailoring molecular structure and crystalline morphology. *J. Mater. Chem. C 1*, 5818–5832.

(8) Egelhaaf, H.-J., Gierschner, J., and Oelkrug, D. (2002) Polarizability effects and energy transfer in quinquethiophene doped bithiophene and OPV films. *Synth. Met. 127*, 221–227.

(9) Absorption spectra of the crystalline solid could not be obtained because of the inhomogeneity of the samples.

(10) It should be noted however, that for such weakly coupled systems, quantum-chemical calculations are usually ambiguous; thus, the results will depend sensitively on the method applied.

(11) Yoon, S.-J., Chung, J. W., Gierschner, J., Kim, K. S., Choi, M.-G., Kim, D., and Park, S. Y. (2010) Multistimuli two-color luminescence switching via different slip-stacking of highly fluorescent molecular sheets. *J. Am. Chem. Soc. 132*, 13675–13683.

(12) Gierschner, J., Lüer, L., Milián-Medina, B., Oelkrug, D., and Egelhaaf, H.-J. (2013) Highly Emissive H-Aggregates or Aggregation-Induced Emission Quenching? The Photophysics of All-Trans para -Distyrylbenzene. *J. Phys. Chem. Lett. 4*, 2686–2697.

(13) Gierschner, J., Mack, H.-G., Oelkrug, D., Waldner, I., and Rau, H. (2004) Modeling of the Optical Properties of Cofacial Chromophore Pairs: Stilbenophane. *J. Phys. Chem. A 108*, 257–263.